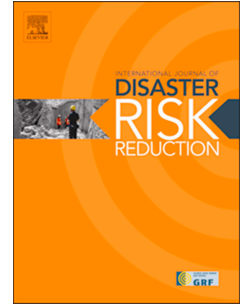


Journal Pre-proof

Regional vulnerability and risk assessment accounting for local building typologies

Maria Polese, Marco Di Ludovico, Marco Gaetani d'Aragona, Andrea Prota, Gaetano Manfredi



PII: S2212-4209(19)30495-9

DOI: <https://doi.org/10.1016/j.ijdr.2019.101400>

Reference: IJDRR 101400

To appear in: *International Journal of Disaster Risk Reduction*

Received Date: 23 April 2019

Revised Date: 15 November 2019

Accepted Date: 17 November 2019

Please cite this article as: M. Polese, M. Di Ludovico, M. Gaetani d'Aragona, A. Prota, G. Manfredi, Regional vulnerability and risk assessment accounting for local building typologies, *International Journal of Disaster Risk Reduction* (2019), doi: <https://doi.org/10.1016/j.ijdr.2019.101400>.

This is a PDF file of an article that has undergone enhancements after acceptance, such as the addition of a cover page and metadata, and formatting for readability, but it is not yet the definitive version of record. This version will undergo additional copyediting, typesetting and review before it is published in its final form, but we are providing this version to give early visibility of the article. Please note that, during the production process, errors may be discovered which could affect the content, and all legal disclaimers that apply to the journal pertain.

© 2019 Published by Elsevier Ltd.

Regional vulnerability and risk assessment accounting for local building typologies

Maria Polese*, Marco Di Ludovico, Marco Gaetani d'Aragona, Andrea Prota and Gaetano

Manfredi

Department of Structures for Engineering and Architecture, University of Naples Federico II, Italy

ABSTRACT

Seismic risk analysis allows investigating the consequences of earthquakes in a region of interest. Most of the existing risk-oriented studies focus on new developments and/or on the integration of most up-to-date information in the fields of seismic hazard evaluation and vulnerability assessment. Conversely, no specific effort was devolved on evaluating the influence of exposure modeling; most of the studies rely on census data at the municipal level for the development of building inventory. Building inventory may change if more information on vulnerability factors for building typologies is considered and this may lead to a different estimation of losses with respect to those based on traditional inventories relying on census data alone. The recent Cartis approach, based on interview, represents an advancement for compilation of regional scale inventories; it allows to rapidly acquire much more data on building typologies with respect to census returns. This paper explores the issue of exposure modeling by comparing the seismic risk computed at the regional scale starting from variable knowledge levels of the building environment. It will be shown that the seismic risk computed starting from the enhanced exposure modeling is generally higher with respect to the standard census-based one. The seismic risk can be nearly doubled for some towns, and the variation is more significant for smaller towns (with smaller number of inhabitants). This result may have a significant influence on evaluations that are based on comparative risk analysis at the regional scale, conditioning decisions towards risk mitigations campaigns or calibration of insurance premiums.

Keywords: inventory; vulnerability; building typology; seismic risk; census; Cartis

* Corresponding author:

Maria Polese, Associate Professor

Department of Structures for Engineering and Architecture

University of Naples Federico II

via Claudio 21, 80125 Naples, Italy

mail: maria.polese@unina.it

tel. +39-0817683485; fax. +39-0817685921

1. INTRODUCTION

Seismic risk analysis is probably the most appropriate tool for investigating the consequences of earthquakes in a region of interest, particularly when the purpose is planning and preparation of long-term risk reduction policies. Indeed, with this analysis approach, entailing the convolution of the seismic hazard with vulnerability and exposure of the assets at risk, all the seismic sources affecting the region are considered and the relative probability of potential earthquakes striking the area in a given time interval is effectively considered. This “integral” approach allows objective comparison among the results for different municipalities in the studied region suitably accounting for all the components of seismic risk, including hazard.

Several studies performed nation-wide or urban level risk assessments adopting macro-seismic intensity scales to represent seismic hazard (e.g. [1]-[4], among other). More recently, quantitative intensity measures such as peak ground motion acceleration PGA^1 or spectral acceleration $Sa(T)$ at the fundamental period T were adopted for characterization of seismic hazard, e.g. [5]-[9]. The focus in the latter studies was in the integration of the most up-to-date information in the fields of seismic hazard evaluation and vulnerability assessment [5]-[8], or in the development of specific risk targeted indicators at the municipal level based on suitable seismogenic model for each analyzed area [9]. Results of seismic risk analysis have been already used in the past to establish repartition of funds for seismic risk reduction [10]-[11] or for planning of risk mitigation campaigns [12]-[13]. Also, risk studies are adopted as benchmark evaluations facilitating the calibration of insurance premiums for buildings [14]-[15]. Therefore, the proper consideration of local building features at the territorial scale is a key aspect in the scope of rational risk reduction programs.

On the other hand, no specific effort in past risk studies was devolved on the exposure side of the problem, with most of the studies simply relying on census data at the municipal level to characterize the building stock towards territorial risk assessment. Recognizing the lack of reliable exposure data for the entire Italian territory, in [16] typological seismic risk maps were derived.

There exists different type of models for assessment of seismic vulnerability for buildings and main ones may be classified as empirical and analytical. Former ones derive vulnerability functions based

¹ List of abbreviations:

A_{Mj} , A_{RCj} = the built area of the j^{th} M or RC building class, respectively

A_T = the total built area in a town

CE = Census-based inventory (and/or related results)

CC = integrated Census+Cartis inventory (and/or related results)

CF = correction factor for seismic risk modification

CU = unit cost ($\text{€}/\text{m}^2$) including technical expenses and VAT;

C_a = altimetric class of the town; C_{pop} = population class of the town

C_s = seismic class of the town (according to [54])

d_m = mean value of damage over the entire municipality

$d_{m,6-9}$ = mean value of d_m in the intensity range $I=6-9$

ERD = earthquake resistant design; M = masonry; RC = reinforced concrete

L = seismic risk expressed in terms of direct economic losses

L_{CE} = seismic risk L calculated starting from CE inventory

L_{CC} = seismic risk L calculated starting from CC inventory

$\Delta L = L_{\text{CC}}/L_{\text{CE}}$ ratio of losses calculated using CC or CE inventory

NT = Number of towns; N_{pop} = population number residing in the sample towns

PGA = peak ground acceleration

$Sa(T)$ = spectral acceleration at the fundamental period T of the structure

V = vulnerability index; ΔV = variation of vulnerability index

VF = vulnerability factor

TS = town statistics; ST = sample towns; TC = town compartment;

$\mu_{D,1}$ = represents the mean damage of the discrete damage distribution at intensity I

$\Delta\mu_{D,6-9}$ = variation of $\mu_{D,1}$, due to the variation ΔV , averaged for intensities 6 to 9

on the statistical treatment of observed damage after past earthquakes (e.g. [2],[17]-[21]), while the latter evaluate seismic fragility curves relying on building modeling and simulation-based assessment of building damage due to earthquakes (e.g. [22]-[28]).

Concerning building inventory, the simpler approach is the one proposed by the European macro-seismic scale EMS-98 [29], where the only parameter needed to classify buildings is material of the lateral load resisting system. However, several models for assessment of seismic vulnerability consider additional information on significant building features, as e.g. construction age or the type of horizontal system, to obtain a significant classification for vulnerability assessment ([17],[20],[30]-[31]). Such kind of information may be achieved with building-by-building survey, that is costly and time consuming and is therefore typically applied only during post-earthquake vulnerability and damage survey campaigns or to integrate and/or verify poor data in benchmark studies of spatially limited areas, e.g. for selected town districts (e.g. [32]).

For large scale assessments, the inventory is frequently based on census data, which are cheap sources of information available over a large scale and dispatched in aggregated form (i.e. for group of buildings) for geo-localized cells. Considering European countries, the information on buildings from census returns is often limited to construction age and storey number [33]. Therefore, the basic census information is often integrated by more or less rapid in situ surveys (e.g. by external visual screening) for the evaluation of earthquake scenarios at the town level ([32], [34]-[37]). For larger scale assessments, e.g. at regional or even national scale, other integrative approaches to increase the information available in building inventory should be used. Innovative image-processing based techniques, using high resolution (HR) optical satellite imagery or from airborne radar sensors, are attractive due to their rapidity and automation and the potential spread over large regions of interest [38]. However, parameters that are more important for vulnerability assessment, such as building materials or the type of horizontal system, cannot be established based on earth observation data alone. Therefore, other techniques should be applied. In [39]-[40] data-mining approaches were proposed. In [2]- [41], statistical studies based on post-earthquake damage data were performed to propose correlations between the structural elements used, and hence the vulnerability class, with the age of masonry buildings. This way a census-based classification can be transformed to a classification relevant to vulnerability.

The recent interview-based Cartis approach [42], developed in Italy in the framework of “Territorial themes” ReLUIS project, financed by Italian National Civil Protection Department, supports the compilation of regional scale inventories. The Cartis form is normally compiled for an entire town, suitably subdividing it in Town Compartments TC. For each TC, the form is filled by interviewing expert technicians with relevant knowledge of building features in the area and collecting information on relevant building typologies in each TC. Such information is more detailed with respect to the data available from census returns and supports effective use of more refined vulnerability models. More than 300 towns in Italy were investigated with the Cartis approach and the data were uploaded a suitable web application allowing the consultation of data from the scientific community (<https://cartis.plinivis.it>). In [43] the information collected through the Cartis form was used to improve building inventory according to three different vulnerability models [19]-[20],[31]. The paper proposed an approach to combine the information available in Census database with additional data gathered with the Cartis form and demonstrated its usefulness with an application for a town in southern Italy. However, an estimation of the variation of the vulnerability and consequently of the impact at the regional scale is still missing.

This paper exploits the results of Cartis-based survey and evaluates the effect of adopting an enhanced exposure assessment on the estimation of seismic risk at the regional scale. Differently from other examples of large-scale risk assessments, the focus is on the effects of improved building inventory, accounting for local territorial-specific building features, on the possible differentiation of building vulnerability within a region and on the resulting variation of seismic risk.

In this work, a sample of 26 towns for which the Cartis form is compiled, covering nearly 10% of the population in Campania region, is studied, evaluating the variation of mean town vulnerability and total annual risk considering or not the additional information from Cartis. It will be shown that such variation depends on the population class C_{pop} of the town (see section 4 for description of C_{pop}) and generally decrease with increasing C_{pop} . Hence, suitable correction factors are calibrated varying C_{pop} . The global risk, in terms of direct economic losses, is firstly estimated for the towns of whole the region starting from census-based building inventory (CE). To this end, the IRMA platform for computation of seismic risk, developed by Eucentre, was employed [44]. Next, applying the correction factors to each town, depending on C_{pop} , the global risk is modified to obtain a new estimate accounting for region-specific building features. It will be shown that annual seismic risk can result nearly doubled for smaller towns, those having smaller population, while for medium-large ones an increase of nearly 20%, if territorial-specific building features are considered, can be expected.

2 SEISMIC VULNERABILITY FOR ORDINARY BUILDINGS

In this study, we employ the RISK-UE vulnerability model [31] to evaluate the susceptibility of ordinary, residential, buildings to earthquakes and estimate the damage distribution after seismic events of assigned intensity. A recent advancement of the model was proposed in [44]; however, for the purpose of the present investigation, we refer to the original model, that is quite established and already extensively applied in literature ([45]-[48]). The RISK-UE model employs the macro-seismic method, that measures the seismic vulnerability in terms of a vulnerability index V and of a ductility index Q , both evaluated taking into account the building typology and its constructive features. The damage scale used in the model is the one defined in EMS98 [29]. Five +1 damage grades D_k ($k = 0...5$), including no damage, are defined in the scale considering the damage observed for both structural and non-structural components. The hazard is described in terms of the EMS-98 macro-seismic intensity I , which is considered as a continuous parameter evaluated with respect to a rigid soil condition; amplification effects due to different soil conditions can be considered with a suitable variation of the vulnerability parameter V .

In the RISK-UE model, preliminary classification of buildings depends only on the construction material and basic information on the vertical structural system (masonry M or reinforced concrete RC type) according to the EMS-98 approach. In particular, 7 building types made of masonry (M1 rubble stone; M2 adobe – earth bricks; M3 simple stone; M4 massive stone; M5 unreinforced masonry – old bricks; M6 unreinforced masonry – RC floors; M7 reinforced/confined masonry) and 3 of reinforced concrete (RC1 concrete moment frames; RC2 concrete shear walls; RC3 dual system) are identified; the level of earthquake resistant design ERD for RC buildings is also considered. Adopting a fuzzy-random approach, the authors transform the numerical linguistic assignments of the EMS-98 scale into numerical values, deriving basic assignments of vulnerability index V^* as well as ranges of V values corresponding to probable (V/V^+) and less probable (V^-/V^{++}) behavior for 13 building typologies. As example, Table 1 reports the Building Typology Matrix BTM, extracted from [31], with the V ranges associated to buildings belonging to typologies M3, M4 and RC1 without ERD or with moderate ERD.

The correlation between the seismic input and the expected damage is expressed in terms of vulnerability curves depending on the assessed vulnerability, described by a closed analytical function:

$$\mu_{D,I} = 2.5 \left[1 + \tanh \left(\frac{I + 6.25V - 13.1}{Q} \right) \right] \quad (1)$$

In eq. (1) the mean damage $\mu_{D,I}$ increases with the macro-seismic intensity I and depends on the vulnerability V ; the parameter Q controls the slope of the curves and may assume different values depending on building typology. As observed in [31], a value of $Q=2.3$ may be assumed to be representative for masonry buildings not specifically designed to have ductile behavior and also for reinforced concrete buildings without ERD or with low level of ERD.

Table 1. Vulnerability index values V for several cases of the building typology matrix, BTM (adapted from [31])

Typology	Description	Vulnerability indices				
		V^-	V^-	V^*	V^+	V^{++}
M3	Unreinforced masonry bearing walls - simple stone	0.46	0.65	0.74	0.83	1.02
M4	Unreinforced masonry bearing walls - massive stone	0.3	0.49	0.616	0.793	0.86
RC1	RC frame (without ERD)	0.3	0.49	0.644	0.8	1.02
	RC frame (moderate ERD)	0.14	0.33	0.484	0.64	0.86

The probability $p_{k/I}$ of obtaining a damage level k , due to an event of intensity I , may be derived as a function of the mean damage and assuming a binomial distribution [31]. Hence, given V for a building typology, it is possible to calculate the fragility curves for the different damage states, i.e. the probability of attaining assigned damage levels varying earthquake intensities (in this case the macro-seismic intensity I). To represent the fragility in terms of peak ground acceleration PGA , objectively measurable after earthquakes, that is the intensity parameter used in the IRMA platform, suitable (I - PGA) correlations should be adopted. Several proposals may be found in literature (e.g. [49]-[50]). In this paper the formula proposed in [31] was adopted:

$$PGA = c_1 c_2^{(I-5)} \quad (2)$$

with $c_1=0.03$ and $c_2=1.6$.

2.1 The influence of vulnerability factors on seismic vulnerability

The basic information contained in census databases allow to classify buildings based on construction material (masonry, reinforced concrete or other), storey number and construction age ranges. The information on construction age, coupled with the year of seismic classification for a municipality, allows to determine whether the building was designed according to seismic regulations or not and the level of ERD. Therefore, starting from census-based data, and making some assumptions on the type of masonry (e.g. if simple stone M3, unreinforced masonry -old bricks - M5 etc.) or on the type of horizontal loads bearing system for RC (frames or walls), it is possible to attribute initial V^* value for the building typology and to fully define the building inventory according to the RISK-UE model.

If additional information is available, it is possible to improve the vulnerability characterization for the generic building adopting Eq. (3):

$$V = V^* + \Delta V \quad (3)$$

with V final vulnerability index, ΔV behavior modifier score, accounting for the effect of relevant vulnerability factors VF s. In [31] two additional score modifiers were introduced, namely ΔV_r , regional modifier, accounting for possible evidence of better or worst performance of buildings in a region with respect to that established for the corresponding typology in the macro-seismic method and ΔV_s , soil amplification modifier, accounting for possible different site effects with respect to rigid soil. However in this paper, with the aim of investigating the effect of the presence of different VF s, only behavior modifier scores are considered.

For example, additional VF s such as e.g. building position in the block or regularity in plan or elevation, can be explicitly considered to modify the building vulnerability [51].

Table 2, adapted from [51], resumes the ΔV values considered as vulnerability modifiers for different VF s and referring to M and RC buildings, respectively. Only the VF considered in the present study are shown in Table 2, while the complete list of possible modifiers may be found in [51]. Note that the ΔV due to horizontal structure type (for M buildings) is also included in Table 2, inferring the ΔV values from the V values assigned in [31].

As it can be seen, according to the parameters under investigation, the maximum variation ΔV for M buildings is due to storey height variation (from ME to LO or to HI), presence of vaults or presence/absence of retrofitting interventions (± 0.08), while for RC buildings the maximum ΔV is due to preservation state and plan or elevation irregularity (+0.04).

Table 2. The vulnerabilities modifiers for different VF s (adapted from [31])

Vulnerability modifiers	Masonry M	ΔV	Reinforced Concrete RC	ΔV
State of preservation	Good state	-0.04	Good state	+0.0
	Bad state	+0.04	Bad state	+0.04
Ns	LO (1, 2)	-0.08	LO (1, 2, 3)	-0.02
	ME (3, 4, 5)	+0.0	ME (4, 5, 6, 7)	+0.0
	HI (≥ 6)	+0.08	HI (≥ 8)	+0.0
Plan irregularity	yes	+0.04	yes	+0.04
Elevation irregularity	yes	+0.04	yes	+0.04
Retrofit intervention	yes	-0.08		
	no	+0.08		
Horizontal structure	steel slabs	-0.06		
	wood slabs	-0.02		
	vaults	+0.08		

Due to the non-linearity of Eq. (1), the effect of the same positive or negative variation of V is non symmetric in the estimation of μ_D ; considering the range of intensities 6÷9, that represents an I interval where more damage observations are available [52], generally a positive ΔV determines a higher variation of μ_D with respect to a negative ΔV .

3 METODOLOGY TO BUILD INTEGRATED BUILDING INVENTORY

The primary source for building inventory at the large scale are census data-bases. ISTAT data [53], in Italy, provide several information for each census tract, including the number of residential buildings, the storey number, the age of construction and the main material of vertical structures (RC, M or other). However, for privacy reason, the data are made available only in aggregated form. For example, it is not directly possible to distinguish buildings by material (RC or M) and contemporarily by construction age and storey number. In [43] a simple procedure was introduced that, relying on available statistics at the provincial level on the age distribution of M and RC buildings, and applying basic de-aggregation rules, allows to disaggregate the data available for each single census tract. In this paper, a slightly modified procedure is applied. The proposed improvement takes advantage on the availability, through the IRMA platform [44], of disaggregated data concerning age-storey distribution for both M and RC buildings (and related surface areas) in each town; this way, suitable town-level marginal distributions of storey number (from 1 to 8), for assigned age intervals (<1919; '19-'45; '46-'61; '62-'71; '72-'81; '82-'91; > 1991), can be built for each town, avoiding rougher estimates based on statistics available only at the province level. Fig. 1 synthetizes the steps to obtain census-based (CE) building inventory. Basic input data are census data for each census tract, the mentioned town marginal distributions (town statistics TS) and information on local context, allowing e.g. to establish the prevalent quality of masonry type.

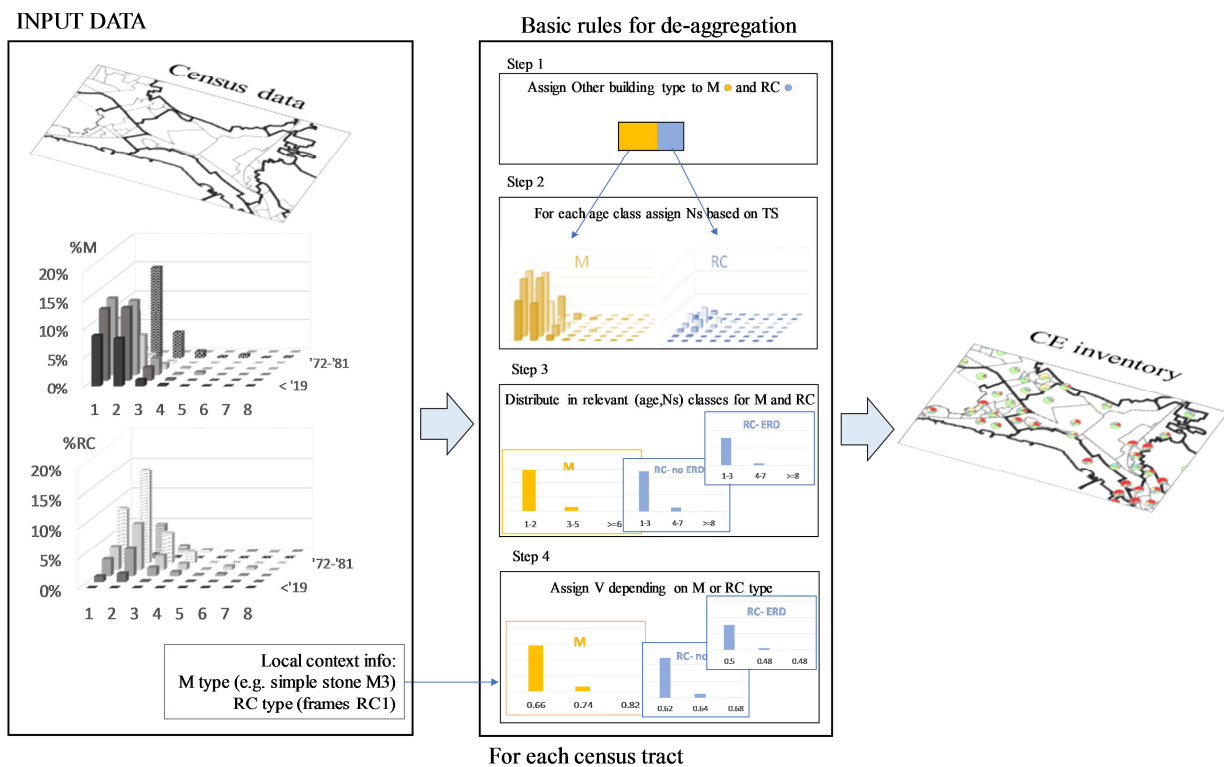


Fig. 1 – Schematic representation of the process to build census-based CE inventory

The goal of the procedure is to obtain, for each census tract, the number of M and RC buildings and their distribution in suitable height and age ranges, so that relevant vulnerability factors depending on building typology could be assigned. For each census tract the number of residential buildings categorized as “Other” is firstly assigned to M and RC based on relevant percentage distribution of the two materials in the same census tract (Step 1). Next, based on the TS, the M and RC buildings are subdivided in storey number Ns (from 1 to 8) for each age range (Step 2). Finally (Step 3), the (age, Ns) buildings are grouped in height ranges according to the RISK-UE proposal for M and RC

buildings, i.e. in LO (Ns 1/2), ME (3/5) and HI (6+) for M buildings or LO (Ns 1/3), ME (4/7) and HI (8+) for RC ones; note that RC buildings are also subdivided according to ERD level, if the town is seismically classified, depending on the age range and the year of first classification of the town. The final identification of each building typology depends on the quality of masonry type (e.g. simple stone M3 or bricks M5) or type of RC structure (frame RC1 or walls RC2). In Italy RC buildings are mostly frame type, so RC1 typology is predominant. For M buildings, the type depends on the region and on availability of different type of stones in different areas.

A common M type in Campania region is simple stone M3 (made of squared tuff blocks). Having chosen the M and RC type, the corresponding V values can be assigned (step 4). Repeating the steps 1 to 4 for all the census tracts in the town, the inventory is finalized and the CE inventory is obtained as output of the procedure. Note that also total building surface area distribution in age-storey ranges, for both M and RC buildings, is available through the IRMA platform; therefore, following the same procedure adopted to subdivide buildings in relevant typologies assigning the relative V , also the corresponding global surface is attributed. The knowledge of the global surface area pertaining to each typology, indicated as A_{Mj} or A_{RCj} for the generic j^{th} M or RC typology, is necessary to compute expected losses depending on damage distribution (see section 4.3).

Building inventory can be enhanced if additional information on VFs is considered. As discussed in section 1, different approaches could be used to gather additional information on building features, such as in-situ surveys for small scale studies or image-processing based techniques and/or data-mining approaches for larger scale assessments. In this paper we refer to the interview-based Cartis survey form as possible source to integrate the building inventory towards regional scale vulnerability and risk assessments. However, in principle, any other source providing the required information on relevant parameters could be used in place of the Cartis form. Fig. 2, adapted from [43], synthesizes the steps to obtain integrated Census+Cartis (CC) building inventory. The relative percentage incidence of each building typology identified in the Cartis form, as well as the data characterizing it (the VFs), are given at the level of each town compartment TC in which the town is subdivided. Therefore, the first operation to combine the information available in census database and in the Cartis form is to identify the census tracts belonging to each TC (Step 1); if some of the census tracts belong to more TCs the percentage incidence of their area in each compartment is evaluated by map superimposition in GIS. Next, considering all the census tracts belonging to a TC, and applying the same de-aggregation rules described before, the number of buildings belonging to each (age-Ns) class is evaluated for all the census tracts belonging to the TC and finally assembled to obtain (age-Ns) classes at the level of the compartment (Step 2). Next, the information available in the Cartis form is applied to the buildings in the TC. Firstly, the % distribution of buildings in the relevant M and RC typologies that are present in the TC is assigned (Step 3); note that each typology identified in the Cartis form is characterized also by the type (type of masonry, e.g. simple stone or bricks, for M or type of structural system, e.g. frame or walls, for RC). The combination of the (age-Ns) classes obtained at step 2 with the % incidence of typologies (type of M and of RC) of step 3 allows to obtain a first distribution of sub-classes (corresponding to building typologies in each TC) and of the associated V parameter at the TC level. Next, a further modification of vulnerability index is applied to all the obtained sub-classes of the compartment. Indeed, the information on relevant VFs and on their percental incidence within each sub-class, obtained thanks to the Cartis form, allows to identify relevant sub-typologies in a TC as well as the number of buildings belonging to each of them; applying Eq. (3), a final V value $V=V^*+\Delta V$ is obtained for each sub-typology (step 4). Note that the final V for a sub-typology is computed simply summing up the vulnerability index and score modifiers, while the number of buildings to which each final V is

referred, i.e. the buildings of the sub-typology to which the ΔV s are applied, depends on the percentage of buildings in the considered typology that is characterized by the corresponding VFs .

Repeating the steps 1 to 4 for all the TC in the town the CC inventory, including also global surface area pertaining to each M and RC typology at the town level, is finalized.

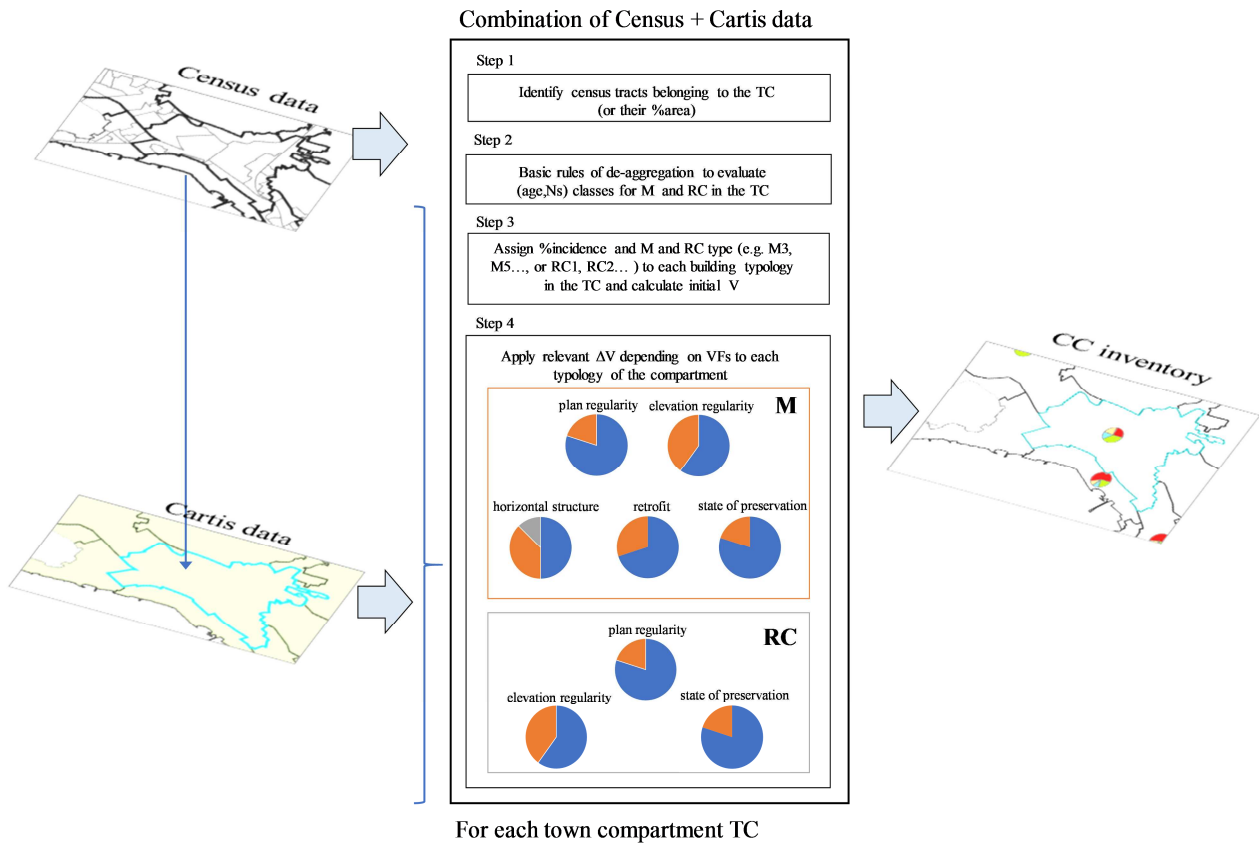


Fig. 2 – Schematic representation of the process to build CC inventory (adapted from [43])

The reliability of the obtained building inventory depends on the amount and quality of the information used to categorize buildings into relevant vulnerability classes, that for the case of Cartis approach depends on the expertise of the interviewed technician(s). Possible errors in vulnerability factors attributions and miss-classification may occur and this obviously influences the results in terms of final vulnerability and risk evaluations. More refined approaches to enhance building inventory could be used leading to more controlled information on the building features, e.g. via building-by building survey. However, such detailed building survey is too costly and time-consuming for large scale analyses and therefore simpler, faster and more affordable approaches, even if affected by larger errors, are needed.

4 APPLICATION IN CAMPANIA REGION - SOUTHERN ITALY

The proposed methodology to build census-based CE and integrated census+Cartis based inventory CC is applied to 26 towns in Campania region (Italy), listed in Table 3, for which the Cartis form was compiled. The meanings of abbreviations are reported in the relevant list, note 1. Columns M and RC reports the number of masonry and RC buildings in the town, already including the buildings made of “other” material attributed to M or RC as explained in section 3. Fig. 3 shows the individuation of TCs for a sample town as well as the typologies individuated in each TC with the

Cartis form; contour of single census tracts can be noted as marked lines in each TC. Some of the characteristics detected for one of the building typologies in a TC are also reported as example. Note that the typologies (denominated MUR for M buildings and CAR for RC buildings), do not correspond to the typologies and distribution obtained with CC inventory because the latter take into account the further sub-categorization considering the possible *VF*s (each Cartis typology may be characterized by one or more *VF*s) and is assembled at the town level.

Table 3. The sample towns in Campania region*

Town	C _{pop}	C _a	C _s	M	RC	Town	C _{pop}	C _a	C _s	M	RC
Agerola	4	4	3	1072	875	Lettere	4	4	3	403	487
Agropoli	5	4	3	2169	1529	Liveri	2	5	2	261	112
Alife	4	3	2	1758	405	Piano di Sorrento	5	4	3	886	444
Angri	5	5	2	1838	1743	Pollena Trocchia	5	4	2	1070	455
Aversa	6	5	2	1739	1795	Pompei	5	5	2	1631	2136
Bacoli	5	4	2	3019	1103	Portici**	6	4	2	922	870
Bonea	2	1	2	383	22	Pozzuoli	6	4	2	3357	3260
Calvanico	2	3	2	205	120	San Potito Sannitico	2	1	1	595	62
Casamarciano	3	3	2	418	101	San Tammaro	3	5	2	498	289
Casola di Napoli	3	4	3	255	279	Sant'Agnello	4	4	3	504	482
Cicerale	2	3	3	538	50	Sant'Anastasia	5	4	2	1792	1393
Frasso Telesino	3	1	2	815	36	Solopaca	3	1	2	1028	303
Gragnano	5	4	3	1047	1240	Vietri sul Mare	4	4	3	682	315

* M and RC buildings include “Other” in [53] (subdivided based on relative percentages of materials in each town)

**for the town of Portici only a portion of the town (~86% of buildings and 96% of population) is considered

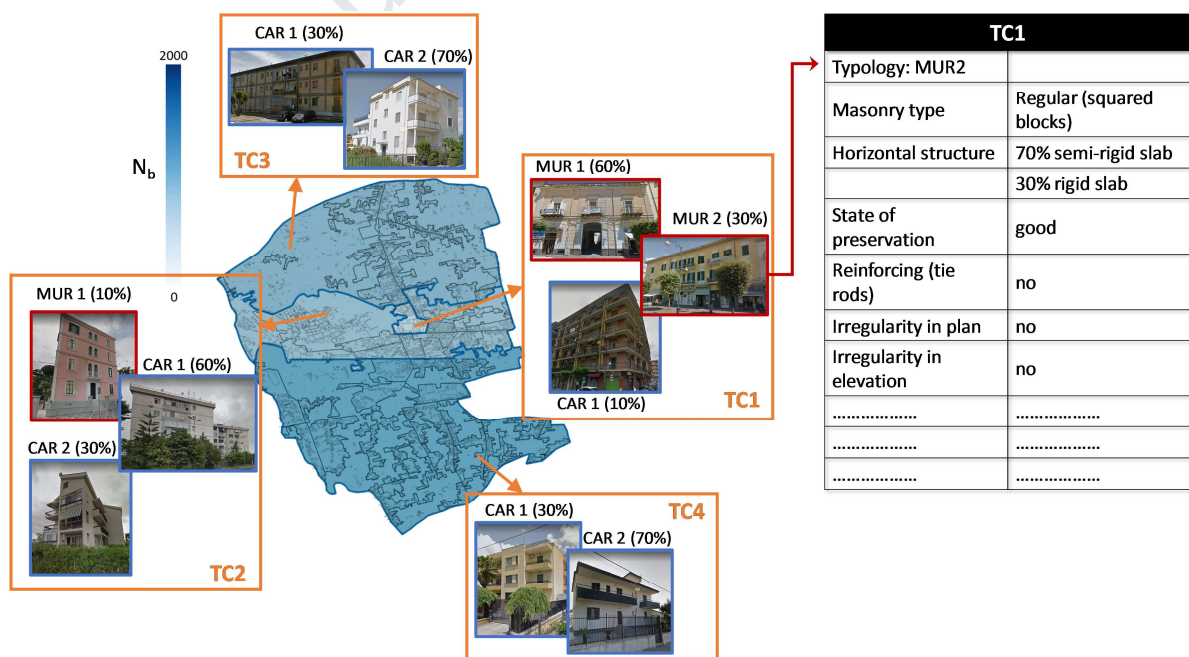


Fig. 3 –Individuation of TCs for a town and the relative building typologies. The characteristics of a building typology in a TC are also reported as example

According to the ISTAT classification in different C_{pop} population ranges [53] (<500, $C_{pop}=1$; 501-2000, $C_{pop}=2$; 2001-5000, $C_{pop}=3$; 5001-10000, $C_{pop}=4$; 10001-50000, $C_{pop}=5$; 50001-250000, $C_{pop}=6$; >250000, $C_{pop}=7$), the 26 sample towns belong to C_{pop} from 2 to 6 (see Fig. 4 (a), contour of the towns are evidenced as black lines in the map).

Also, they belong to different altimetric classes C_a (internal mountain, $C_a=1$; mountain near the coast, $C_a=2$; internal hill, $C_a=3$; hill near the coast, $C_a=4$; plain, $C_a=5$), see Fig. 4 (b), and to different seismic zones according to [54], see Fig. 4 (c).

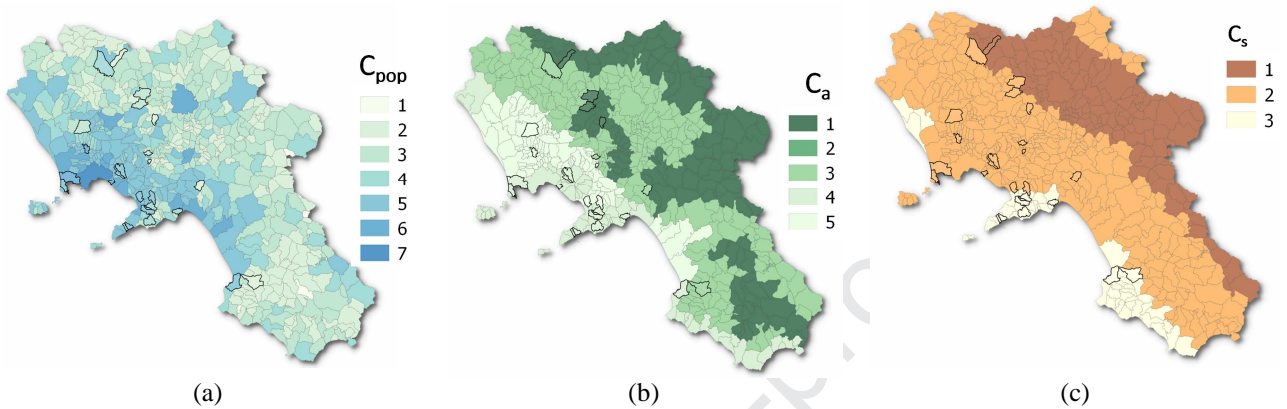


Fig. 4 – Campania region with identification of the sample towns and (a) C_{pop} classes; (b) C_a classes; (c) seismic zones C_s according to [54]

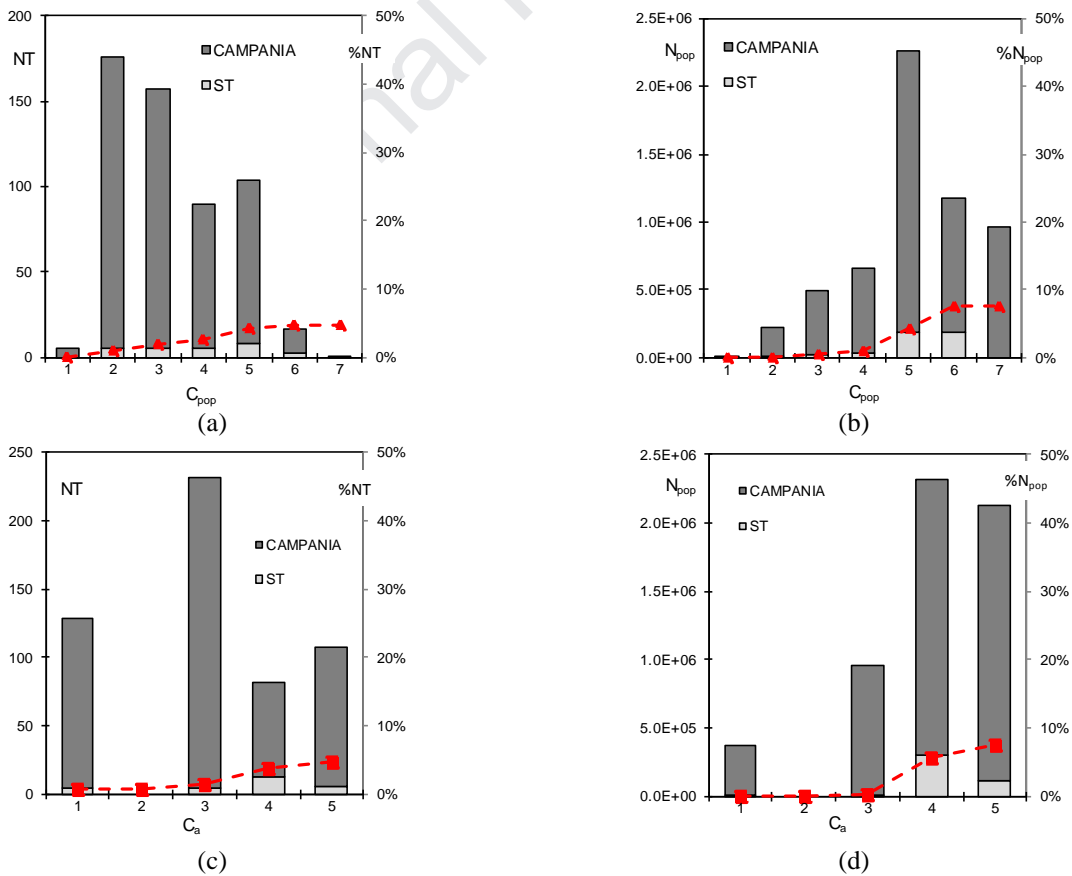


Fig. 5 – Number of towns NT and percentage distribution of the sample towns %NT with respect to Campania region as a function of population class C_{pop} (a) and altimetric class C_a (c); population number residing in the sample towns N_{pop} and % distribution of inhabitants $\%N_{pop}$ with respect to Campania region as a function of C_{pop} (b) and C_a (d)

The sample towns ST (26 towns) represent about 5% of the number of towns (%NT) in Campania region, see gray histograms and red dashed line in Fig. 5 (a) which reports the cumulative trend of %NT as a function of C_{pop} . Small towns, that are the most numerous in Campania region, are represented in the ST as a lower percentage ($\sim 3\%$ of Campania region towns with $C_{pop}=2$) with respect to larger ones ($\sim 18\%$ of Campania region towns with $C_{pop}=6$). In terms of population (percentage $\%N_{pop}$) the global representativeness of ST increases up to 8% of the number of Campania inhabitants (see red dashed line in Fig. 5 (b)). The representativeness of ST in the classes $C_{pop}=2$ and $C_{pop}=6$ achieve 4% and 16%, respectively.

Very small centers, with less than 500 inhabitants ($C_{pop}=1$), as well as the only metropolis in the region (that is Naples, $C_{pop} = 7$) are not represented in the ST database. The distribution of ST in altimetric classes gives lower value 3% for internal mountain $C_a=1$, while the towns in $C_a=4$ (hill near the coast) are the most represented (16%), see light gray histograms with respect to dark gray ones in Fig. 5 (c). In terms of population the percentages vary from 1.4% (for $C_a=3$) to 13% (for $C_a=4$).

4.1 Census based (CE) and integrated Census+Cartis (CC) building inventory

Applying the procedures described in section 3 both the CE and CC inventories are obtained for the 26 sample towns. The vulnerability factor V obtained at the end of the procedure accounting for ΔV ranges from 0.36 (for RC1 buildings) to 1.02 (for M1 buildings); therefore, a synthetic representation of inventory is not straightforward. To allow an easier representation of the inventory, the buildings belonging to relevant V ranges are assigned to selected vulnerability classes. V ranges are established based on membership functions defined in [31] to represent the vulnerability classes introduced in EMS-98 [29] and the following association is adopted: A: $0.82 \leq V$; B: $0.66 \leq V < 0.82$; C: $0.5 \leq V < 0.66$; D: $0.34 \leq V < 0.5$. As example, Fig. 6 (a)-(b)-(c)-(d)-(e) show the CE and CC inventory, represented as percentage of buildings belonging to each vulnerability class, for 5 of the sample towns, one for each C_{pop} under investigation.

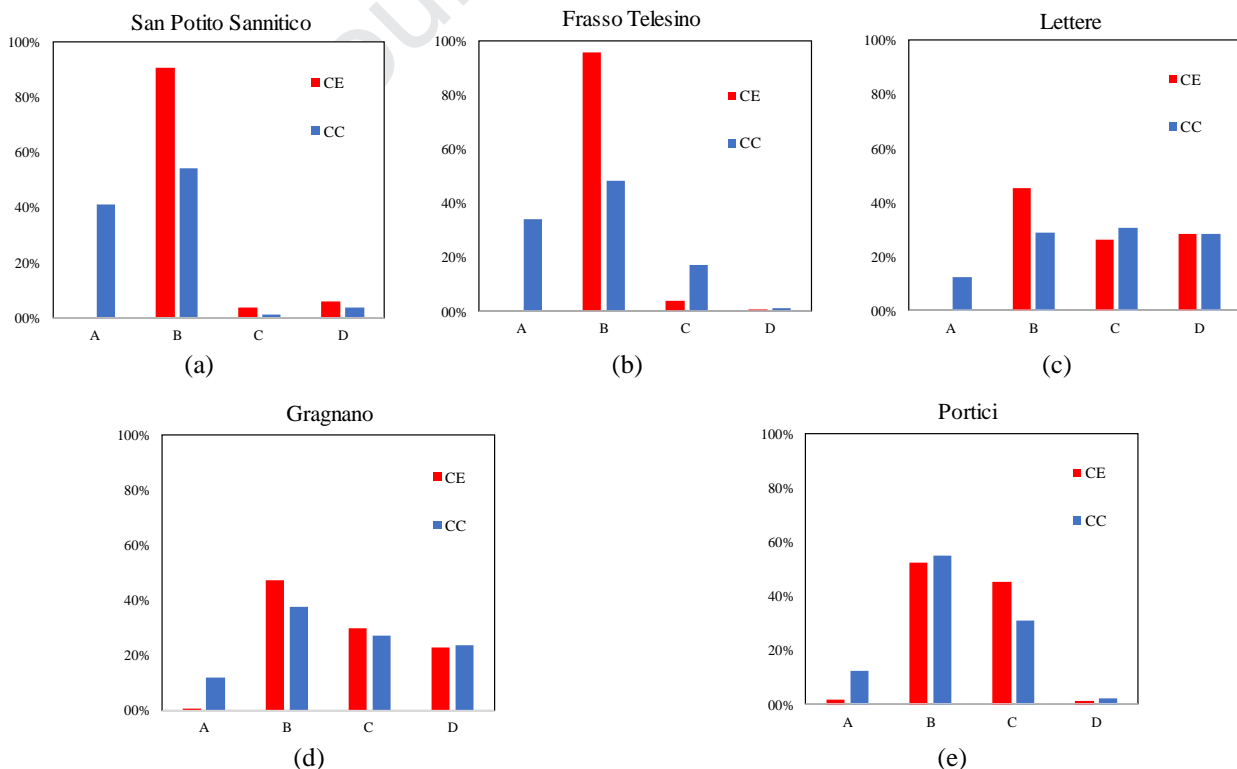


Fig. 6 – CE and CC inventory represented as %buildings in vulnerability classes from A to D for the towns of (a) San Potito Sannitico; (b) Frasso Telesino; (c) Lettere; (d) Gragnano; (e) Portici

As it can be noted, the distribution of vulnerability classes can change significantly from CE to CC inventory. For example, referring to the town of San Potito Sannitico (Fig. 6 (a)), more than 90% of the buildings are classified in B with CE inventory, while with CC inventory approximately one half of those buildings are re-classified, with final distribution of about 50% buildings in B and more than 40% in A. Apparently, the changes of inventory are more significant for smaller towns, e.g. for San Potito Sannitico having $C_{pop}=2$ or Frasso Telesino with $C_{pop}=3$, with respect to larger ones, e.g. for Gragnano with $C_{pop}=5$ or Portici with $C_{pop}=6$. The next section investigates on possible correlations of vulnerability with C_{pop} and C_a of the sample towns.

4.2 Variation of vulnerability at the town level

A first observation on the vulnerability for a town arises considering the percental distribution of M and RC buildings in the town. RC buildings have generally lower vulnerability with respect to M ones, as evidenced also by the comparatively lower V values attributed to RC typologies (see e.g. Table 1). Hence, it is expected that towns with higher percentage of M buildings %M will be characterized by a larger mean vulnerability with respect to those having lower %M. Fig. 7 (a) and (b) show the mean distribution of %M and %RC for the towns as a function of C_{pop} and C_a , respectively. As it can be seen, smaller towns tend to have a higher %M with respect to those having higher C_{pop} (Fig. 7 (a)). Hence, it could be expected a higher mean vulnerability for smaller towns. Similarly, the towns in lower altimetric class (those that are higher with respect to the sea level, e.g. internal mountains or high hills) have a higher %M with respect to the towns that are in plain areas. As a matter of fact, the towns in mountain or internal hilly territory are often also the smaller ones, and it is possible to establish an almost linear correlation between population and altimetric class, C_{pop} and C_a . Therefore, considering the correlation of C_a with C_{pop} , in the elaborations to follow only the variation with C_{pop} will be explicitly investigated.

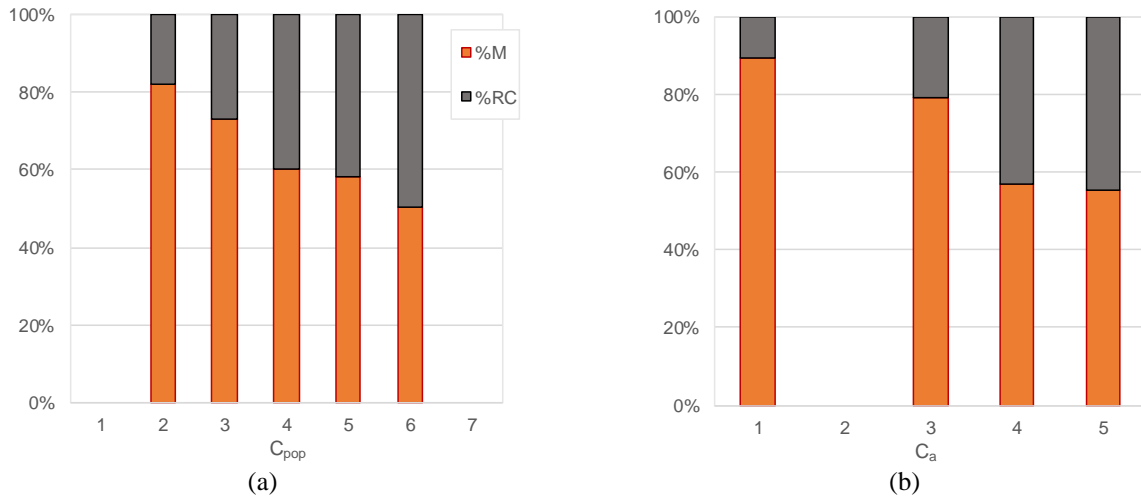


Fig. 7 – Variation of %M for the sample towns (a) and mean %M and %RC in the towns (b) as a function of C_{pop}

The building inventory obtained for each town is used to estimate a mean value of damage over the entire municipality d_m , calculated with Eq. (4):

$$d_m(I) = \frac{1}{5} \sum_{k=0}^5 \left(\frac{N_{k|I}}{N_{tot}} \cdot k \right) \quad (4)$$

with N_{tot} the number of buildings in the municipality, k the damage level and $N_{k/I}$ the number of buildings having damage level k at seismic intensity I . The mean value of d_m in the intensity range $I=6\div 9$, $d_{m,6-9}$, is used as a synthetic parameter to represent building vulnerability at the town level. The mean damage d_m is calculated starting from building typologies distribution obtained with both the CE and CC inventories; obviously, starting from different inventories also the resulting d_m changes. Fig. 8 (a) shows the variation of $d_{m,6-9}$ with C_{pop} for both the CE and the CC cases. As it can be observed, the CC based $d_{m,6-9}$ is generally greater with respect to the one corresponding to CE inventory and d_m shows a slightly decreasing trend with C_{pop} . This trend confirms what already observed based on greater %M for smaller towns. The higher vulnerability for smaller towns was also observed in [3]. Fig. 8 (b) shows the variation of the ratio of mean damage indices $\Delta d_{m,6-9}=(d_{m,6-9})_{CC}/(d_{m,6-9})_{CE}$ with C_{pop} ; it can be noted that $\Delta d_{m,6-9}$ is generally higher for the towns of lower C_{pop} , and a decreasing trend with C_{pop} is observed. This trend confirms what was expected based on the higher %M for smaller towns

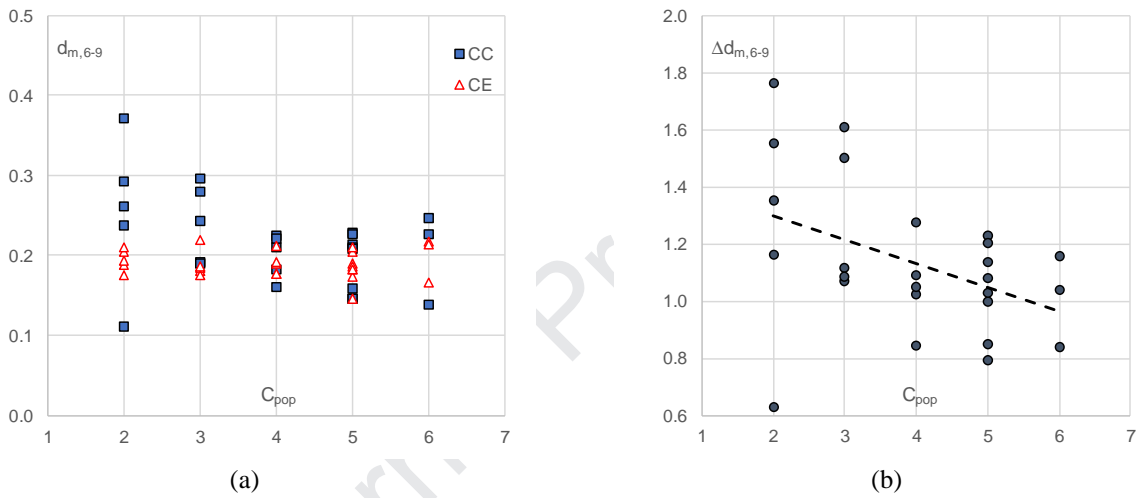


Fig. 8 – Variation of $d_{m,6-9}$ obtained starting from CE and the CC inventories (a) and of the ratio $\Delta d_{m,6-9}$ (b) with C_{pop}

4.3 Variation of seismic risk at the town level

Seismic risk expressed in terms of direct economic losses for each town may be computed with Eq. (5) [44]:

$$L=CU \left(\sum_{j=1}^{n_M} \sum_{k=1}^5 A_{Mj} P_{Mj,k} C_k + \sum_{j=1}^{n_{RC}} \sum_{k=1}^5 A_{RCj} P_{RCj,k} C_k \right) \quad (5)$$

with n_M , n_{RC} = number of M and RC building classes, respectively; CU = Unit cost ($\text{€}/\text{m}^2$) including technical expenses and not including VAT; A_{Mj} , A_{RCj} = the built area of the j^{th} M or RC building class, respectively; $p_{Mj,k}$, $p_{RCj,k}$ = the probability, in the considered time frame t for risk estimation, for the j^{th} M or RC building class to experience structural damage state k ; c_k = percentage cost of repair or replacement (with respect to CU) for each structural damage state k . The cost parameters adopted in Eq. (6) are calibrated based on the actual repair costs that were monitored in the reconstruction process following recent Italian earthquakes [55]-[56]. In particular, $CU=1350$ ($\text{€}/\text{m}^2$) is adopted and, to account for uncertainty in the estimation, two sets of values of cost percentages (%min and %max) related to different damage states are considered for the analyses: $c_{1,min}=2\%$, $c_{2,min}=10\%$, $c_{3,min}=30\%$, $c_{4,min}=60\%$ and $c_{5,min}=100\%$; $c_{1,max}=5\%$, $c_{2,max}=20\%$, $c_{3,max}=45\%$, $c_{4,max}=80\%$ and $c_{5,max}=100\%$.

The generic probability p_k of attaining damage state k in t years (the subscript M_j or RC_j are not indicated for brevity reason) is calculated as a function of the mean annual rate of damage λ_k , assuming that the occurrence of earthquakes follows a Poisson process:

$$p_k \text{ (in } t \text{ years)} = 1 - e^{-\lambda_k t} \quad (6)$$

The rate λ_k , representing the risk of attaining damage state D_k , is expressed as:

$$\lambda_k = \int_0^{\infty} P(D_k | im) \cdot |d\lambda_{IM}(im)| \quad (7)$$

with $P(D_k | im)$ the probability that the structure will attain damage state D_k when subjected to an earthquake with ground motion intensity level im , and λ_{IM} the mean annual frequency of exceedance of the ground motion intensity im . Hence, the λ_k (and p_k) for the generic building typology in a town depends on seismic hazard at the site and on the seismic fragility at damage state D_k for the considered building typology. For small values of λ_k and $t=1$ the approximation $p_k \approx \lambda_k$ holds [57].

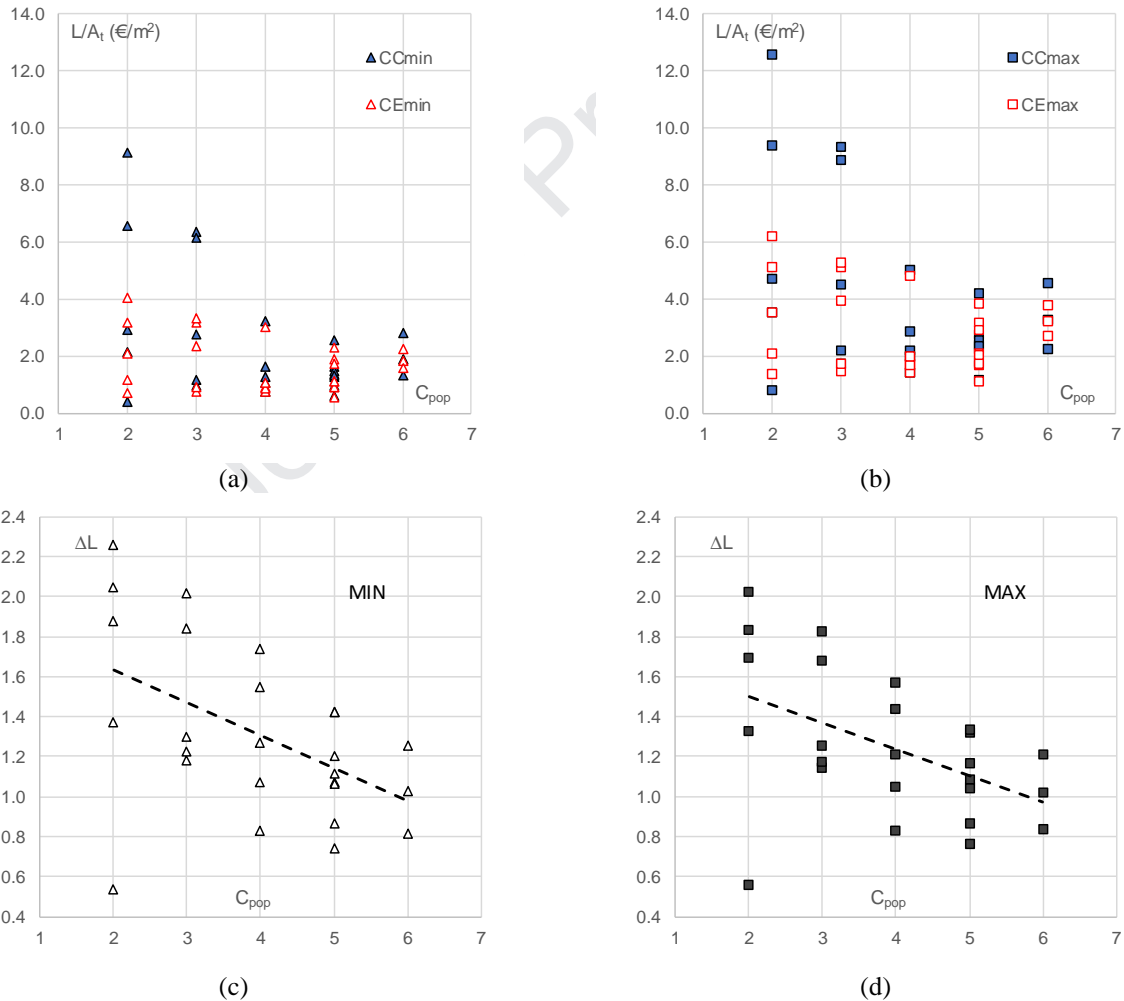


Fig. 9 – Variation of L/A_t (€/m²) obtained starting from CE and the CC inventories and considering % min (a) or % max (b) cost percentages; variation of the ratio ΔL with C_{pop} for the %min (c) or %max (d) cost percentages.

Having completed the building inventory (both CE and CC) for all the 26 sample towns, the building typological classes, and the relative fragility curves for the adopted vulnerability model,

are available in each town, together with the A_{Mj} , A_{RCj} associated to each M or RC building class. The seismic hazard is available for all the territory in Italy [58], hence all the ingredients for calculation of seismic risk as in Eq. (5) are available. Fig. 9 (a)-(b) shows the variation with C_{pop} of total annual risk L ($t=1$), normalized by the total built area of each town A_t , for both the CE and the CC cases and considering both %min and %max for the cost percentages. Coherently with the trends on mean damage observed in Fig. 9 (a), also the (normalized) losses computed starting from CC inventory are larger with respect to the ones computed starting from CE inventory. Fig. 9 (c)-(d) shows the variation of the ratio of losses calculated using CC or CE inventory $\Delta L=L_{CC}/L_{CE}$ with C_{pop} , again for both the %min and %max cost percentages; similarly to Fig. 9 (b) it can be noted that ΔL is generally higher for the towns of lower C_{pop} (up to about two times), and a decreasing trend with C_{pop} is observed. However, the variation of L_{CC} and L_{CE} within the towns is not only due to the variation of towns vulnerability, as represented by $d_{m,6-9}$. In fact, the ST are also characterized by very different seismic hazard, as can be observed already in Fig. 4 (c). Therefore, the variation of expected annual losses depends both on the vulnerability of the town and on the seismic hazard at the site.

5 REGIONAL BASED VULNERABILITY AND RISK ESTIMATION

The seismic vulnerability and risk for the entire Campania region is computed with the aid of the IRMA platform [44]. In IRMA the damage assessment and/or risk calculation is performed using OpenQuake, the calculation engine developed by Global Earthquake Model (GEM) www.globalquakemodel.org. In IRMA the census database is preloaded with data disaggregated at the town level; hence, given the suitable exposure/vulnerability rules corresponding to the chosen vulnerability model, e.g. RISK-UE [31], the building inventory based on census data [53], corresponding to CE inventory, is automatically built. The fragility curves in IRMA are lognormal cumulative distribution functions defined in terms of PGA. The seismic hazard in IRMA is based on the MPS04 hazard model, developed by INGV and adopted at national level with Civil Protection Ordinance [58].

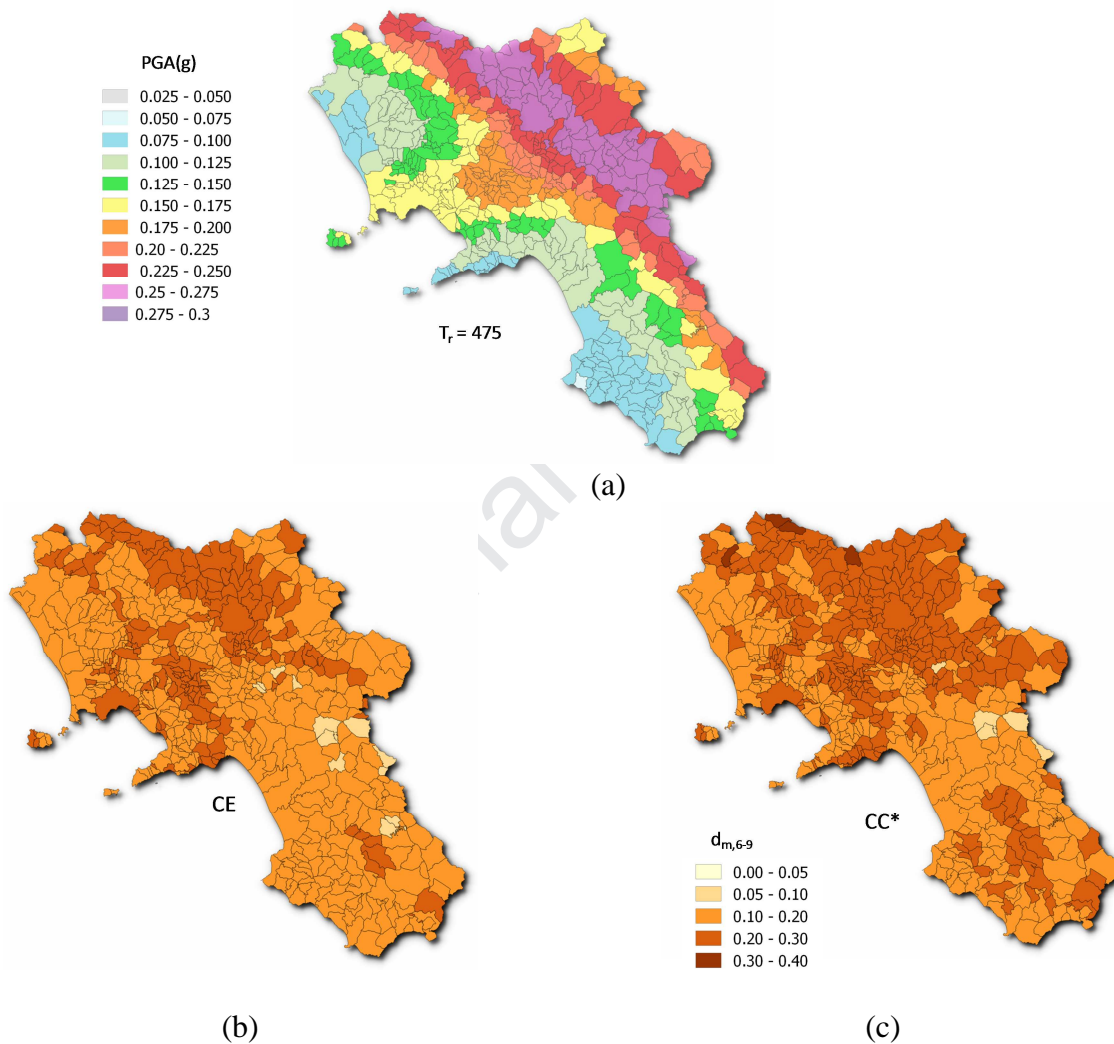
Fig. 10 (a) shows the seismic hazard map for Campania region in terms of PGA for return period $Tr=475$ years.

As for vulnerability map, it may be represented in terms of $d_{m,6-9}$ at the municipality level. The intensity measure in IRMA is expressed in terms of PGA. Therefore, the $d_{m,6-9}$ evaluated for each town, represented in Fig. 10 (b) at the regional scale for Campania region, is evaluated with the aid of IRMA platform by averaging the d_m calculated for the PGAs falling into the intensity interval $I=6\div 8$; this vulnerability map correspond to CE building inventory.

The annual seismic risk was calculated with IRMA adopting the cost parameters introduced in section 4.3 (%min and %max). Fig. 10 (d) shows the map of annual seismic risk for the case of %max cost percentage; the expected losses for each town are expressed normalizing them with respect to the total built area in the town L/A_t ($\text{€}/\text{m}^2$); also in this case, the CE building inventory is considered. The expected annual risk in the region ranges between 0 - 9 $\text{€}/\text{m}^2$ for the case of %min cost percentages (figure not shown for brevity reason) and 0 - 12 $\text{€}/\text{m}^2$ for the case of %max. Calculating the ratio of the losses evaluated for each town adopting the %max coefficients versus the one corresponding to %min, a maximum (minimum) loss variation of more than 100% (50%) is obtained. On average, the expected annual risk is 2.7 $\text{€}/\text{m}^2$ for %min costs and 4.4 $\text{€}/\text{m}^2$ for %max costs, with more than 60% loss variation due to the uncertainty in the cost parameters.

When additional information on building features representing local peculiarities and/or weaknesses towards seismic vulnerability is considered, e.g. through CC inventory, the resulting seismic vulnerability and risk increase.

The variations of $\Delta d_{m,6-9}$ evaluated for the sample towns depending on C_{pop} , see Fig. 8 (b), can be used for calibrating suitable correction factors $CF_v(C_{pop})$ to be applied for preliminary estimations of a modified value of building vulnerability at the town level, accounting for typological features characterizing locally the building environment. Based on the decreasing trend observed in Fig. 8 (b), it is assumed $CF_v(C_{pop}=2)=1.3$, $CF_v(C_{pop}=3)=1.2$, $CF_v(C_{pop}=4)=1.1$, $CF_v(C_{pop}=5)=1.0$, $CF_v(C_{pop}=6)=1.0$. Extrapolating the trend of Fig. 8 (b), for the few towns with $C_{pop}=1$, $CF_v=1.4$ is used; for the city of Naples ($C_{pop}=7$) $CF_v=1.0$ is assumed.



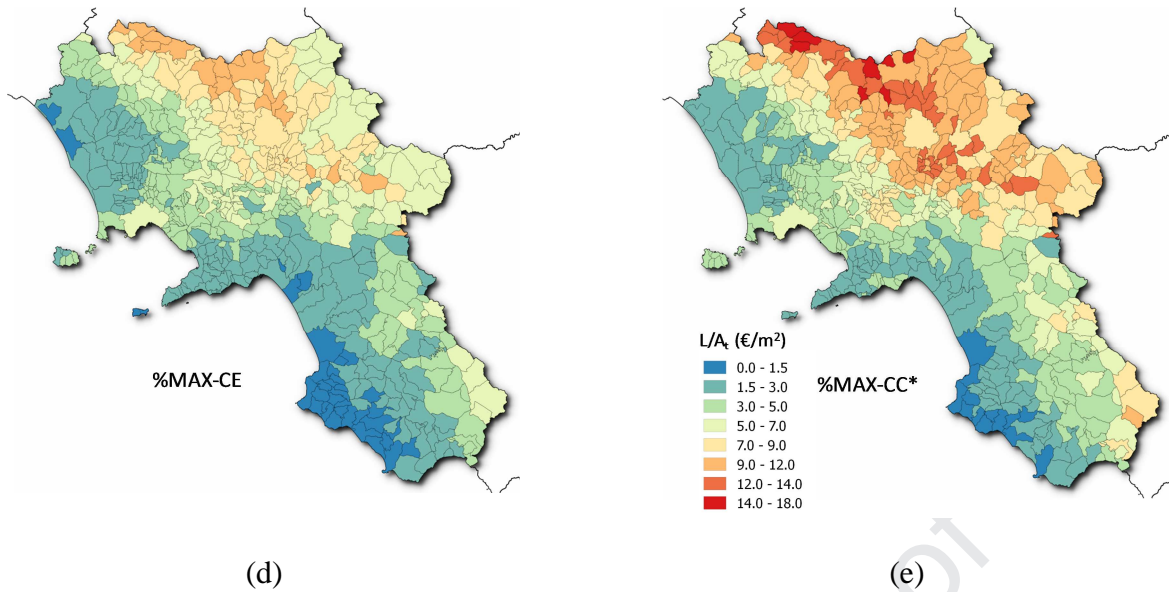


Fig. 10 – Hazard, vulnerability and Risk maps for Campania region: Hazard map in terms of PGA(g) for $T_r=475$ years (a); vulnerability map in terms of $d_{m,6-9}$ based on CE (b); modified vulnerability map obtained applying the $CF_v(C_{pop})$ (c); map of total annual risk (in terms of L/A_i (€/m²) for each town) calculated with %max cost percentage and based on CE (d) inventory; modified risk maps obtained applying the $CF(C_{pop})$ for the case of %max cost percentage (e)

The ST used for calibration of the CF_v represent nearly 10% of the population in Campania region. A sensitivity study performed including more towns [59] showed that the considered sample is sufficiently representative for the calibration of the correction factors. CF_v can be applied to the $d_{m,6-9}$ calculated for all the towns in Campania region with IRMA [44]. This way, new modified vulnerability maps are obtained, as represented in Fig. 10 (c) and denoted as CC*; the asterisk indicates that maps are obtained from those in Fig. 10 (b) by application of the CF_v .

Similarly, the variations of ΔL evaluated for the sample towns depending on C_{pop} , see Fig. 9 (c)-(d), can be used for calibrating suitable correction factors $CF(C_{pop})$ to be applied for preliminary estimations of a modified value of annual seismic risk. Based on the decreasing trend observed in Fig. 9 (c), it is assumed $CF(C_{pop}=2)=1.6$, $CF(C_{pop}=3)=1.5$, $CF(C_{pop}=4)=1.3$, $CF(C_{pop}=5)=1.1$, $CF(C_{pop}=6)=1.0$ for the case of %min cost percentages while CF values 1.5, 1.4, 1.2, 1.1, and 1 are deduced from the decreasing trend observed in Fig. 9 (d) corresponding to %max cost percentages. For $C_{pop}=1$, $CF=1.8$ or 1.6 are obtained for %min and %max by extrapolation of the relative trends. For the city of Naples ($C_{pop}=7$) $CF=1.0$ is assumed for both %min and %max.

CF are applied to the values of annual seismic risk, in terms of L/A_i (€/m²), calculated for all the towns in Campania region with IRMA. The new modified risk map for the case of %max cost percentages is represented in Fig. 10 (e) (denoted as %MAX-CC*); for brevity reason, the modified risk map for %min is not shown. Note that the maximum expected annual risk increases to about 18 €/m² for the case of %max cost percentages; for the case of %min cost percentages the increase is up to 12 €/m² (not shown). On average, the expected annual risk result in 3.8 €/m² for %min costs and 6.0 €/m² for %max costs. This risk increase, that is due to the consideration of typological features characterizing locally the building environment, can reach 60% for some towns and can be locally comparable to the risk increase corresponding to the uncertainty in cost parameters (from %min to %max). By summing up the unconditional expected annual losses, in a 1 year time frame, for all the towns in Campania region, a global amount of approximately 600 million of Euro is obtained when CE inventory is considered (mean value between estimation performed adopting %min and %max cost percentages). Dividing by the total number of buildings in Campania a unit

amount of approximately 730 Euros per building is obtained. Considering that the mean surface area of buildings in Campania is about 230 m^2 , this means that, on average, a yearly loss of about $0.23\% = 730 / (230 \cdot 1350)$ per building could be expected (in 50 year time frame). When the modified risk maps corresponding to CC inventory are used the expected global losses increase to more than 700 million of Euro, corresponding to more than 850 Euros per single building, with a global loss increment higher than 15%.

It is interesting to compare the normalized annual seismic risk, expressed in terms of $(L/A_t)/CU$, with the expected annual loss computed for new buildings, designed with modern codes, according to the guidelines for seismic risk assessment recently introduced in Italy [60]. As observed in [61], the expected annual loss (expressed as a fraction of reconstruction costs) for a new code-conforming building is 1.13%, while the maximum normalized annual risk estimated in the Campania region for existing buildings, $(L/A_t)/CU$, ranges between 1.04% (considering %min cost percentage) and 1.33% (with %max), with a mean value of 1.19%. However, the difference may appear less significant than the expected one because important differences exist between the assumption made in this study and those used for calculation of the expected annual loss recently introduced in Italy in the guidelines for seismic risk classification [60]. The most significant is that the normalized annual risk computed according to guidelines is based on a code compliant approach, which allows assessing losses based on the attainment of conventional limit states rather than on empirical damage. Thus, the estimations are affected by uncertainties due to the correlation between empirical damage and conventional limit state [50] as well as between these parameters and relevant costs [49]. Furthermore, the CU assumed in [60] is $\text{€}1200 \text{ €/m}^2$ while that assumed in the current study is $\text{€}1350 \text{ €/m}^2$ meaning that the normalized annual risk computed in this study should be increased by a factor of 12.5%. This leads to normalized annual risk estimated in the Campania region of 1.17% (considering %min cost percentage) and 1.50% (with %max), with a mean value of 1.33%.

The estimated values of normalized annual risk can be useful for preliminary estimations of the areas where it is more convenient to invest for seismic risk reduction.

6 CONCLUSIONS

This paper investigates on the issue of exposure modeling towards risk assessment at the large scale. The established RISK-UE vulnerability model, allowing to account for different vulnerability factors for the building classification and the estimation of fragility curves, is adopted for characterizing the seismic vulnerability of building typologies. Two levels of building inventory are considered: CE, based on the sole census data available for all the country in Italy, and CC, based on the integration of census data with additional typological information retrieved for several towns. In this paper, the interview-based Cartis approach is adopted as integrative source of information; however, in principle, any other source providing the required information on relevant parameters could be used in place of the Cartis form to obtain CC inventory.

The estimation of town level seismic vulnerability for 26 towns in Campania region, expressed by $d_{m,6-9}$, shows that smaller towns tend to have larger vulnerability and that the estimation based on CC inventory leads to higher mean damage with respect to the one based on CE inventory. Analogous trend is observed for unconditional seismic risk, expressed in terms of annual direct economic losses for a town. Indeed, referring to normalized risk L/A_t , with L the seismic risk expressed in terms of direct economic losses and A_t the total built area for a town, a decreasing trend with increasing population class C_{pop} is observed. Moreover, it is seen that the risk calculated

starting from CC inventory can be nearly doubled with respect to the one obtained from CE inventory for smaller towns. Based on the variation with C_{pop} of the ratio of losses calculated using CC or CE inventory $\Delta L=L_{CC}/L_{CE}$, suitable correction factors CF are calibrated for preliminary estimations of a modified (increased) value of annual seismic risk for the towns in Campania region. Applying such CF to the risk map estimated for Campania starting from inventory based only on census data (CE), modified risk maps accounting for increased knowledge of building features are obtained. Elaborating such results, it is seen that the average unconditional seismic loss in a 1 year time frame for a single building (total losses divided by total building number in the region) increases from approximately 730 Euros per building when CE inventory is considered to more than 850 Euros, with a loss increment of more than 15%. Considering a mean surface area of buildings of about 230 m², this corresponds to a yearly per building loss of about 0.23% for the risk estimated starting from census-based inventory and 0.27% for the risk obtained considering additional building features.

It should be considered that the adopted approach for building inventory, that is oriented to large scale studies at the regional or even national level, allows to obtain a fast and approximate categorization of buildings into vulnerability classes. Obviously, the reliability of the obtained building inventory is influenced by the amount and quality of the information used, and this has a direct effect on the final vulnerability and risk evaluations. Moreover, the obtained results depend on the model adopted to represent the seismic vulnerability for buildings and it is expected that the variations from CE to CC inventory would change if a different vulnerability model is used, as already observed in [43]. Nevertheless, this application at the regional scale allows to have a first quantitative estimation of the effect of adoption of more refined building inventory (even if still simplified and approximate) at the large scale, assessing the increase in expected annual risk, in terms of economic losses. This kind of evaluations may be very useful for preliminary quantifications of seismic insurance premiums in a region.

Acknowledgements

This study was performed in the framework of PE 2019-2021; joint program DPC-Reluis Subproject WP2: Inventory of existing building typologies – CARTIS and WP4: Seismic risk maps and damage scenarios

References

- [1] M.W. Musson, Intensity-based seismic risk assessment, *Soil Dyn. Earthq. Eng.* 20 (2000) 353 – 360.
- [2] Di Pasquale G, Orsini G, Romeo RW, New Developments in Seismic Risk Assessment in Italy, *Bulletin of Earthquake Engineering*, 3 (1), (2005) pp. 101-128
- [3] S. Tyagunov, G. Grunthal, R. Wahlstrom, L. Stempniewski, J. Zschau, Seismic risk mapping for Germany, *Nat. Hazards Earth Syst. Sci.* 6 (4) (2006) 573 – 586.
- [4] K. Pitilakis, M. Alexoudi, S. Argyroudis, A. Anastasiadis, Seismic risk scenarios for an efficient seismic risk management: the case of Thessaloniki (Greece). In *Advances in Earthquake Engineering for Urban Risk Reduction* (2006), (pp. 229-244). Springer, Dordrecht.
- [5] H. Crowley, M. Colombi, B. Borzi, M. Faravelli, M. Onida, M. Lopez, D. Polli, F. Meroni, R. Pinho, A comparison of seismic risk maps for Italy, *Bull. Earthq. Eng.* 7(1) (2009) 149 – 180.

- [6] V. Silva, H. Crowley, H. Varum, R. Pinho, Seismic risk assessment for mainland Portugal. *Bull. Earthq. Eng.*, 13(2) (2015) 429-457.
- [7] H. Chaulagain, H. Rodrigues, V. Silva, E. Spacone, H. Varum, Seismic risk assessment and hazard mapping in Nepal. *Natural Hazards*, 78(1) (2015) 583-602.
- [8] A. J. Kappos, G. Panagopoulos, G. G. Penelis, Development of a seismic damage and loss scenario for contemporary and historical buildings in Thessaloniki, Greece. *Soil Dynamics and Earthquake Engineering*, 28(10-11), (2008) 836-850.
- [9] M. A. Zanini, L. Hofer, C. Pellegrino, A framework for assessing the seismic risk map of Italy and developing a sustainable risk reduction program. *International Journal of Disaster Risk Reduction*, 33 (2019) 74-93.
- [10] Law n. 77/2009, art. 11 (known as “articolo 11”), (2009) downloadable at <https://www.gazzettaufficiale.it/eli/gu/2009/06/27/147/so/99/sg/pdf> (in Italian; last accessed on 11.10.2019)
- [11] Law n. O.P.C.M. 4007/2012 and following ordinances – attachment 2. Repartition of Resources, (2012) downloadable at <https://www.gazzettaufficiale.it/eli/gu/2012/03/07/56/sg/pdf> (in Italian; last accessed on 11.10.2019)
- [12] H. Shakib, S. D. Joghan, M. Pirizadeh, Proposed seismic risk reduction program for the megacity of Tehran, Iran. *Natural Hazards Review*, 12(3), (2011)140-145.
- [13] J. A. Valcárcel, M. G. Mora, O. D. Cardona, L. G. Pujades, A. H. Barbat, G. A. Bernal, Methodology and applications for the benefit cost analysis of the seismic risk reduction in building portfolios at broadscale. *Natural hazards*, 69(1), (2013), 845-868.
- [14] K. A. Porter, J. L. Beck, R. V. Shaikhutdinov, S. K. Au, K. Mizukoshi, M. Miyamura, ...M. Masuda, Effect of seismic risk on lifetime property value. *Earthquake Spectra*, 20(4), (2004), 1211-1237.
- [15] R. Muir-Wood, R. (2011), *Designing Optimal Risk Mitigation and Risk Transfer Mechanisms to Improve the Management of Earthquake Risk in Chile*, OECD Working Papers on Finance, Insurance and Private Pensions, No. 12, (2011) OECD Publishing, Paris
- [16] M. Rota, A. Penna, C. Strobbia, G. Magenes, Typological seismic risk maps for Italy, *Earthq. Spectra* 27 (3) (2011) 907 – 926.
- [17] Braga F, Dolce M, Liberatore D (1982) A statistical study on damaged buildings and an ensuing review of the MSK-76 scale, 1982, In *Proceedings of the seventh European conference on earthquake engineering*, Athens, Greece (pp. 431-450)
- [18] T. Rossetto, A. Elnashai, Derivation of vulnerability functions for European-type RC structures based on observational data, *Engineering Structures*, 25 (2003),1241–1263
- [19] M. Rota, A. Penna, C.L. Strobbia, Processing Italian damage data to derive typological fragility curves. *Soil Dynamics and Earthquake Engineering*, 28 (10-11) (2008), 933-947.
- [20] G. Zuccaro, F. Cacace, Seismic vulnerability assessment based on typological characteristics. The first level procedure “SAVE”, *Soil Dynamics and Earthquake Engineering*, 69 (2015), 262-269
- [21] C. Del Gaudio, G. De Martino, M. Di Ludovico, G. Manfredi, A. Prota, P. Ricci, G.M. Verderame. Empirical fragility curves from damage data on RC buildings after the 2009 L’Aquila earthquake. *Bulletin of Earthquake Engineering*, 15(4), (2017) 1425-1450.

- [22] T. Rossetto, A. Elnashai, A new analytical procedure for the derivation of displacement-based vulnerability curves for populations of RC structures. *Engineering structures*, 27(3) (2005) 397-409.
- [23] B. Borzi, R. Pinho, H. Crowley, Simplified pushover-based vulnerability analysis for large scale assessment of RC buildings. *Engineering Structures*; 30 (3) (2008) 804-820.
- [24] M.A. Erberik Generation of fragility curves for Turkish masonry buildings considering in-plane failure modes. *Earthquake Engineering & Structural Dynamics*, 37(3) (2008) 387-405.
- [25] M. Polese, G.M. Verderame, C. Mariniello, I. Iervolino, G. Manfredi, Vulnerability analysis for gravity load designed RC buildings in Naples–Italy. *Journal of Earthquake Engineering*, 12(S2) (2008) 234-245.
- [26] M. Rota, A. Penna, G. Magenes, A methodology for deriving analytical fragility curves for masonry buildings based on stochastic nonlinear analyses. 2010. *Engineering Structures*, 32(5), (2010), 1312-1323.
- [27] M. Polese, M. Marcolini, G. Zuccaro, F. Cacace, Mechanism Based Assessment of Damaged- Dependent Fragility curves for RC building classes, *Bull Earthquake Eng*, 13 (5), (2015), 1323-1345
- [28] M. Gaetani d’Aragona, M. Polese, K. Elwood, M. Baradaran Shoraka, A. Prota A., Aftershock Collapse Fragility Curves for Non-ductile RC Buildings: A Scenario-based Assessment, *Earthquake Engineering and Structural Dynamics*, 46, (2017), 2083-2102
- [29] G. Grünthal European Macroseismic Scale, *Chaiers du Centre Européen de Géodynamique et de Séismologie*, vol. 15 (1998) Luxembourg
- [30] M. Dolce, A. Masi, M. Marino, M. Vona, Earthquake damage scenarios of the building stock of Potenza (Southern Italy) including site effects. *Bulletin of Earthquake Engineering*, 1(1) (2003) 115-140.
- [31] S. Lagomarsino, S. Giovinazzi, Macroseismic and mechanical models for the vulnerability and damage assessment of current buildings, *Bulletin of Earthquake Engineering* 4 (2006) 415–443
- [32] C. Del Gaudio, P. Ricci, G.M. Verderame, G. Manfredi Development and urban-scale application of a simplified method for seismic fragility assessment of RC buildings. *Engineering Structures*, 91 (2015) 40-57
- [33] H. Crowley, S. Ozcebe, H. Baker, R. Foulser-Piggott, R. Spence, D7.2 State of the knowledge of building inventory data in Europe, *NERA Deliverable*, 7 (2014) v3.
- [34] P. Guéguen, C. Michel, L. LeCorre A simplified approach for vulnerability assessment in moderate-to-low seismic hazard regions: application to Grenoble (France), *Bull Earthq. Engng.*, 4(3) (2007) 467-490
- [35] H. Sucedoğlu, U. Yazgan, A. Yakut, A screening procedure for seismic risk assessment in urban building stocks. *Earthquake Spectra*, 23(2) (2007) 441-458.
- [36] R. Apostolska, G. Necevska-Cvetanovska, V. Shendova, J. Bojadjeva, Seismic performance assessment of “hybrid” structures using two-level multy group GIS oriented approach: case studies. *Bulletin of Earthquake Engineering*, 16(10) (2018) 4797-4824.
- [37] M. Polese, M. Marcolini, M. Gaetani d’Aragona, E. Cosenza Reconstruction policies: explicitating the link of decisions thresholds to safety level and costs for RC buildings, *Bull Earthquake Eng*, 15 (2) (2017) 759-785

- [38] D. Polli, F. Dell'Acqua, P. Gamba First steps towards a framework for earth observation (EO)-based seismic vulnerability evaluation. *Environmental Semeiotics*, 2(1) (2009) 16-30.
- [39] I. Riedel, P. Guéguen, F. Dunand, S. Cottaz Macro-scale vulnerability assessment of cities using Association Rule Learning, *Seismological Research Letters*, 85(2) (2014) 295-305.
- [40] I. Riedel, P. Guéguen, M. Dalla Mura, E. Pathier, T. Leduc, J. Chanussot Seismic Vulnerability assessment of urban environments in moderate-to-low seismic hazard regions using association rule learning and support vector machine methods, *Natural Hazards*, 76(2) (2015) 1111-1141.
- [41] C. Del Gaudio, G. De Martino, M. Di Ludovico, G. Manfredi, A. Prota, P. Ricci, P., & Verderame, G. M. Empirical fragility curves for masonry buildings after the 2009 L'Aquila, Italy, earthquake. *Bulletin of Earthquake Engineering*, (2019), 1-30.
- [42] G. Zuccaro, M. Dolce, D. De Gregorio, E. Speranza, C. Moroni La scheda CARTIS per la caratterizzazione tipologico- strutturale dei comparti urbani costituiti da edifici ordinari. Valutazione dell'esposizione in analisi di rischio sismico, (2015) in proceedings of GNGTS 2015 (in italian)
- [43] M. Polese, M. Gaetani d'Aragona, A. Prota, Simplified approach for building inventory and seismic damage assessment at the territorial scale: an application for a town in southern Italy, *Soil dynamics and earthquake engineering*, 121 (2019) 405-420
- [44] DPC, Italian Civil Protection Department, National risk assessment. Overview of the potential major disasters in Italy: seismic, volcanic, tsunami, hydro-geological/hydraulic and extreme weather, droughts and forest fire risks, (2018), updated December 2018
- [45] N. Lantada, J. Irizarry, A. H. Barbat, X. Goula, A. Roca, T. Susagna, L. G. Pujades, Seismic Hazard and risk scenarios for Barcelona, Spain, using the Risk-UE vulnerability index method. *Bulletin of Earthquake Engineering*, 8 (2), (2010), 201-229.
- [46] S. Cherif, M. Chourak, M. Abed, L. G. Pujades, Seismic risk in the city of Al Hoceima (north of Morocco) using the vulnerability index method, applied in Risk-UE project. *Nat Hazards* (2017) 85:329–347.
- [47] A. Abderrahim, R. D. Driss, A. M. Belhadj, RISK-EU Method applied to the Algerian city of Arzew to assess exposure to earthquakes. *Energy Procedia*, (2017), 139, 236-241.
- [48] J. Ródenas, S. García-Ayllón, A. Tomás, Estimation of the Buildings Seismic Vulnerability: A Methodological Proposal for Planning Ante-Earthquake Scenarios in Urban Areas. *Applied Sciences*, 8(7), (2018),1208.
- [49] C. Margottini, D. Molin, L. Serva, Intensity versus ground motion: A new approach using Italian data, *Engineering Geology*, 33(1) (1992), 45-58
- [50] L. Faenza, A. Michellini, Regression analysis of MCS intensity and ground motion parameters in Italy and its application in ShakeMap. *Geophysical Journal International*, 180(3) (2010) 1138-1152.
- [51] S. Giovinazzi, S. Lagomarsino, A macroseismic method for the vulnerability assessment of buildings. (2004) In Proc. of 13th World Conference on Earthquake Engineering
- [52] G. Zuccaro G Inventory and vulnerability for residential buildings at National territorial level, risk maps and socio-economic losses – Napoli, 2004 (in italian); (2004) CD publishing the results of the Task 1 for SAVE, INGV/GNDT Project, PQ 2000-2002
- [53] ISTAT (2004) Edifici ed abitazioni Censimento 2001. Dati definitivi. (in Italian), released by ISTAT on December 9, 2004 download from dawinci.istat.it

- [54] DGR n. 5447, Delibera Giunta Regionale del 07/11/2002 (2002) in italian, http://www.difesa.suolo.regione.campania.it/component/option,com_remository/Itemid,0/function,fileinfo/id,36/ (accessed on 10.10.2019)
- [55] M. Di Ludovico, A. Prota, C. Moroni, G. Manfredi, M. Dolce, Reconstruction process of damaged residential buildings outside historical centres after the L'Aquila earthquake: Part I—"light damage" reconstruction. *Bull Earthquake Eng.* 15 (2017) 667–692,
- [56] M. Di Ludovico, A. Prota, C. Moroni, G. Manfredi, M. Dolce, Reconstruction process of damaged residential buildings outside historical centres after the L'Aquila earthquake: Part II: "heavy damage" reconstruction. *Bull Earthquake Eng.*, 15 (2017) 693–729
- [57] L. Eads, E. Miranda, H. Krawinkler, D.G. Lignos, An efficient method for estimating the collapse risk of structures in seismic regions *Earthquake Engng Struct. Dyn.* 42(1) (2013) 25–41
- [58] OPCM n.3519 del 28.04.2006 (2006) Criteri generali per l'individuazione delle zone sismiche e per la formazione e l'aggiornamento degli elenchi delle stesse zone. G.U. 11.05.2006 n. 108 (in Italian)
- [59] M. Polese, M. Di Ludovico, A. Prota, G. Tocchi, M. Gaetani d'Aragona, The use of Cartis form for inventory updating and effects on the vulnerability estimations at the territorial scale, XVIII Convegno Nazionale "L'Ingegneria Sismica in Italia", Paper ID 3508, (2019) Ascoli Piceno, Settembre 2019 (in Italian)
- [60] Decreto Ministeriale del 28-02-2017, Approvazione delle Linee guida per la "Classificazione di rischio sismico delle costruzioni" modificato con D.M. n.65 il 7 marzo 2017 (in Italian)
- [61] E. Cosenza, C. Del Vecchio, M. Di Ludovico, M. Dolce, C. Moroni, A. Prota, E. Renzi, The Italian guidelines for seismic risk classification of constructions: technical principles and validation. *Bulletin of Earthquake Engineering*, 16(12) (2018) 5905-5935.
- [62] G.J. O'Reilly, T.J. Sullivan Probabilistic seismic assessment and retrofit considerations for Italian RC frame buildings. *Bull Earth Eng* 16(3) (2018) 1447–1485.

Highlight

- Comparison of regional seismic risk computed with different exposure models
- Enhancement of census-based building inventory with interview-based Cartis approach
- Effect of local building features on inventory and on resulting seismic risk
- Variation of vulnerability at town level depending on the population class of the town

Journal Pre-proof